Heteroatom-induced domain electrostatic potential difference in $ZnIn_2S_4$ nanosheets for efficient charge separation and boosted photocatalytic overall water splitting

Bojing Sun[a‡], Dingge Fan[a‡], Xiaoyu Chen[a], Zhenzi Li[b], Wei Zhou*[b], and Yunchen Du*[a]

[a] MIIT Key Laboratory of Critical Materials Technology for New Energy Conversion and Storage, School of Chemistry and Chemical Engineering, Harbin Institute of Technology, Harbin 150001, China

[b] Shandong Provincial Key Laboratory of Molecular Engineering, School of Chemistry and Chemical Engineering, Qilu University of Technology (Shandong Academy of Sciences), Jinan, Shandong, 250353, China.

---

* *Corresponding authors.*

E-mail address: yunchendu@hit.edu.cn. (Y. Du); zwchem@hotmail.com. (W. Zhou).

Characterization

X-ray diffraction (XRD) measurements were performed by using the Bruker D8 Advance diffractometer by using Cu Kα radiation (λ=1.5406 Å). The transmission electron microscopy (TEM) was obtained on a JEOL-2100 electron microscope (JEOL, Japan) with an acceleration voltage of 200 kV. Nitrogen adsorption-desorption isotherms at 77 K were collected on an AUTOSORB-1 (Quantachrome Instruments) nitrogen adsorption apparatus. All samples were degassed under vacuum at 150 °C for at least 5 h before measurement. UV/vis adsorption spectra were conducted on a UV/vis spectrophotometer (Lambda 950 (PerkinElmer, USA)) in the range of 200-800 nm. X-ray photoelectron spectroscopy (XPS) (thermofisher escalab 250xi) was recorded to study the surface states. The luminescence lifetimes were detected with an Edinburgh FL-FS 920 fluorescence spectrophotometer with an excitation wavelength at 350 nm. The amount of Al doping was measured by Inductively Coupled Plasma (Optima 8300 (PerkinElmer, USA) ICP-OES). The photoluminescence (PL) spectra were measured by a PELS 55 spectrofluoro-photometer with the excitation wavelength of 330 nm.

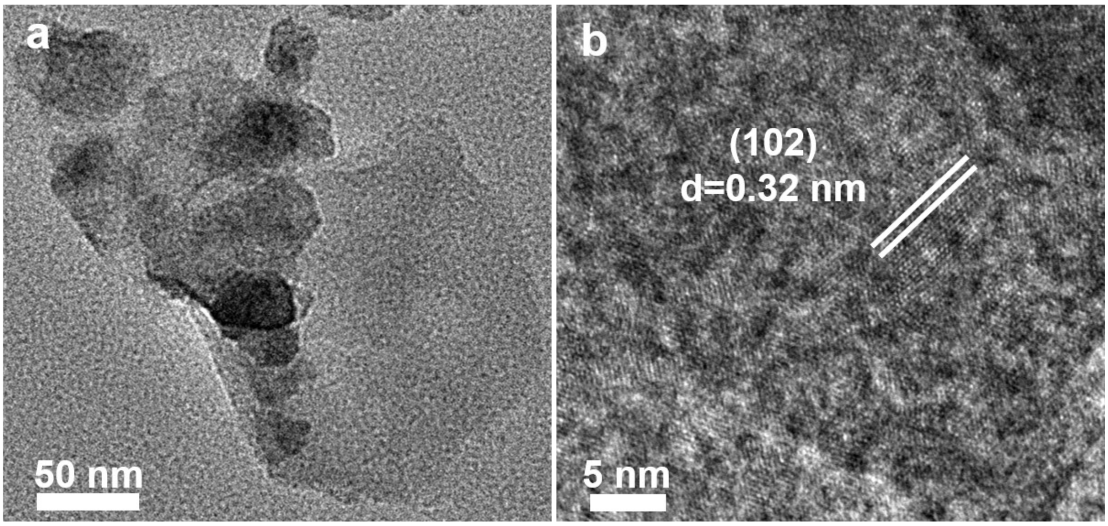

Fig. S1. (a) TEM and (b) HRTEM images of ZIS nanosheets.

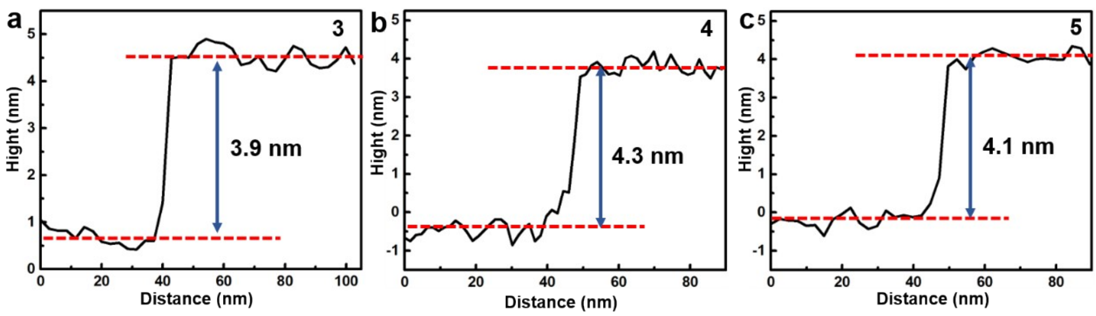

Fig. S2. The corresponding height profiles of Al-ZIS nanosheets.

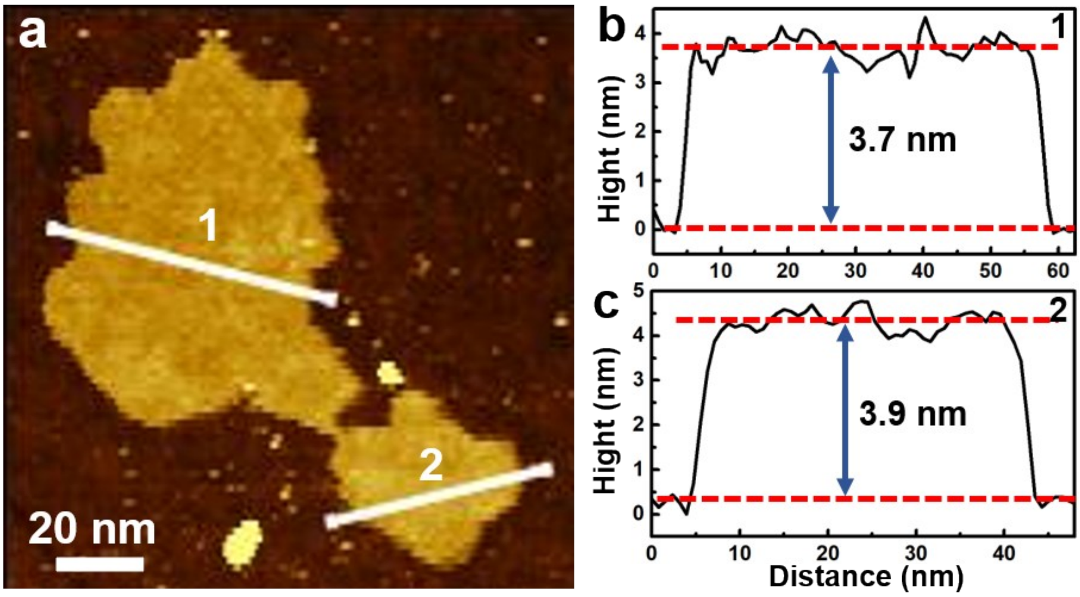

Fig. S3. (a) AFM image and (b) the corresponding height profiles of pure ZIS nanosheets.

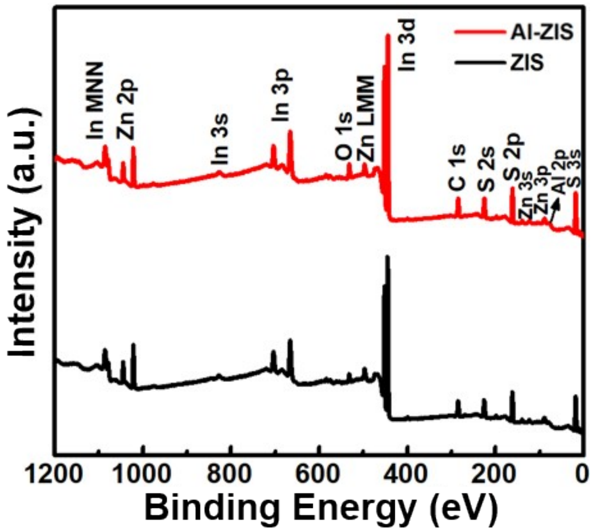

Fig. S4. XPS spectra of full survey for ZIS and Al-ZIS nanosheets, respectively.

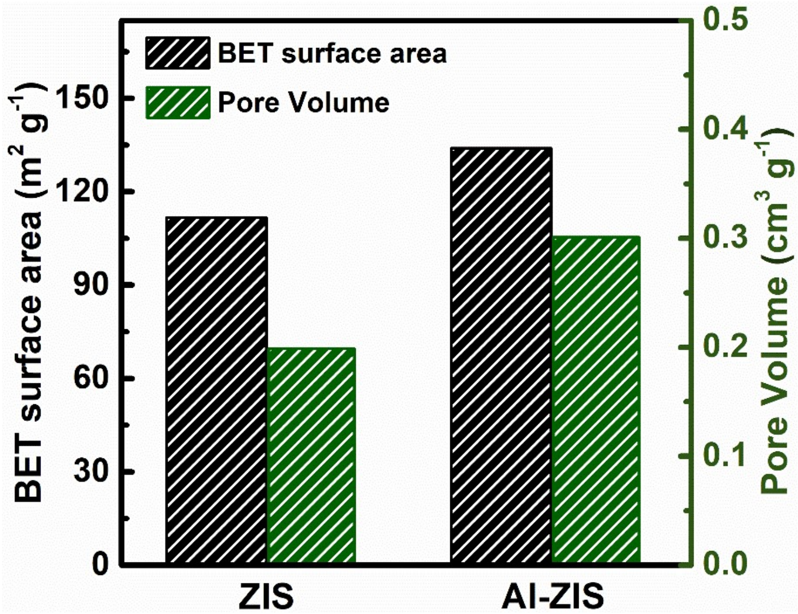

Fig. S5. The BET surface areas and pore volumes of ZIS and Al-ZIS nanosheets.

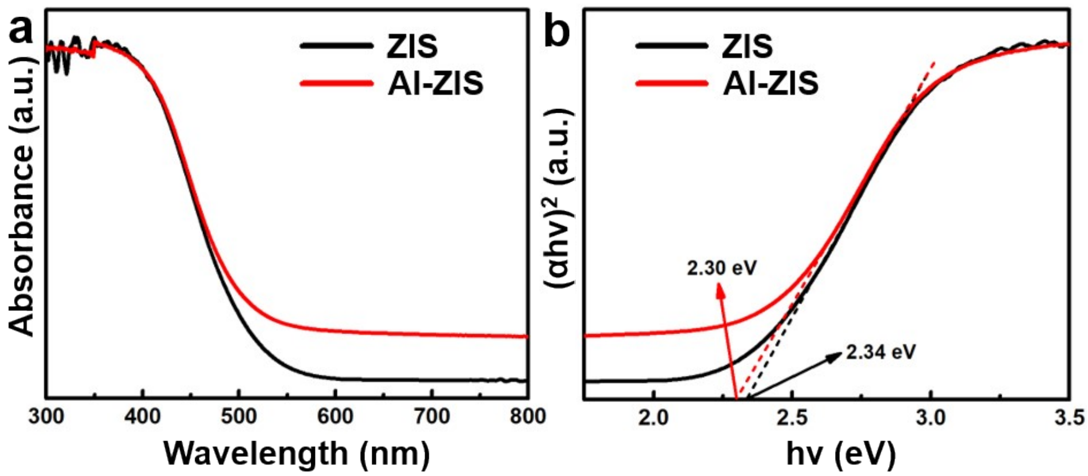

Fig. S6. UV-vis absorption spectra and corresponding bandgaps of ZIS and Al-ZIS nanosheets.

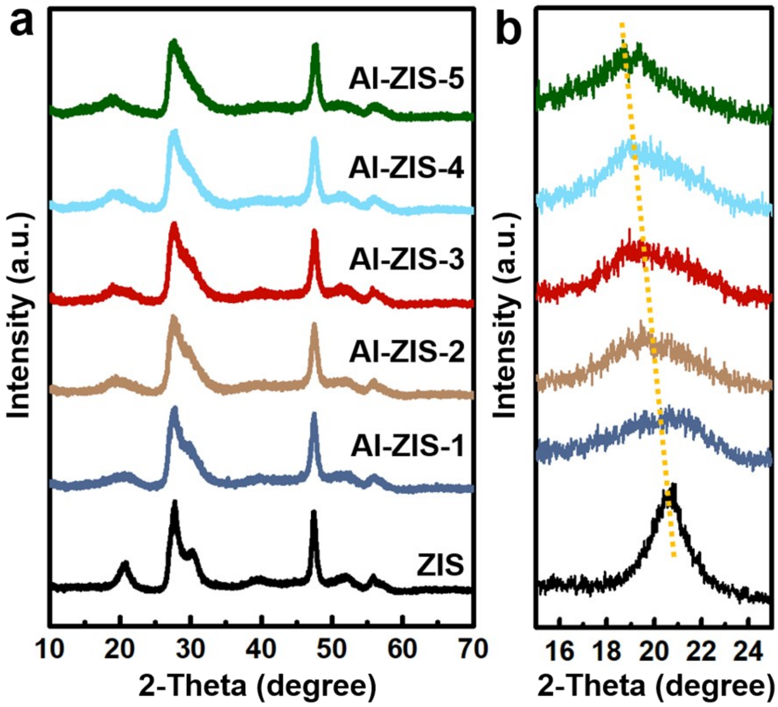

Fig. S7. XRD patterns of Al-ZIS nanosheets with different Al doping amounts.

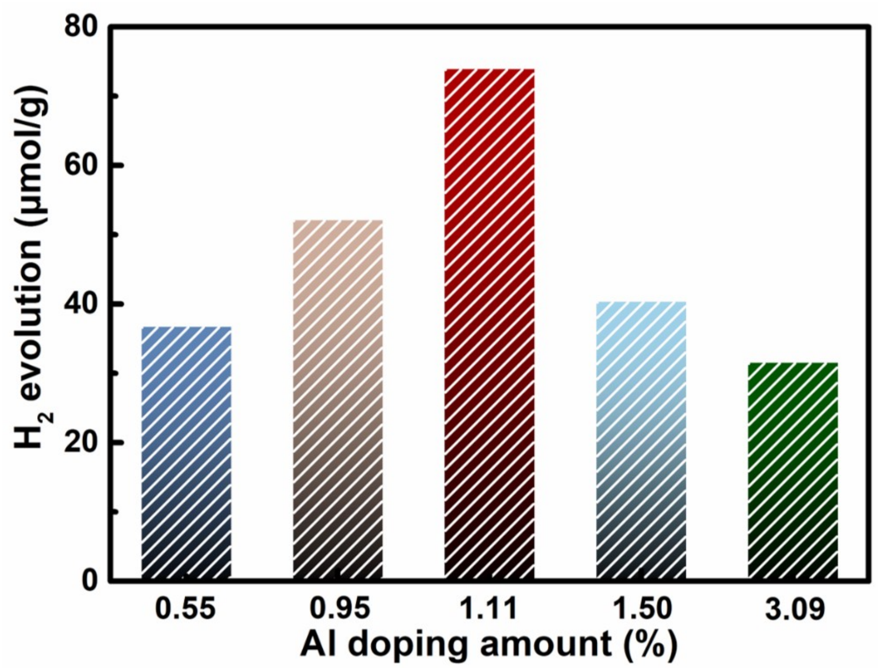

Fig. S8. H_2 evolution rates of Al-ZIS nanosheets with different Al doping amounts.

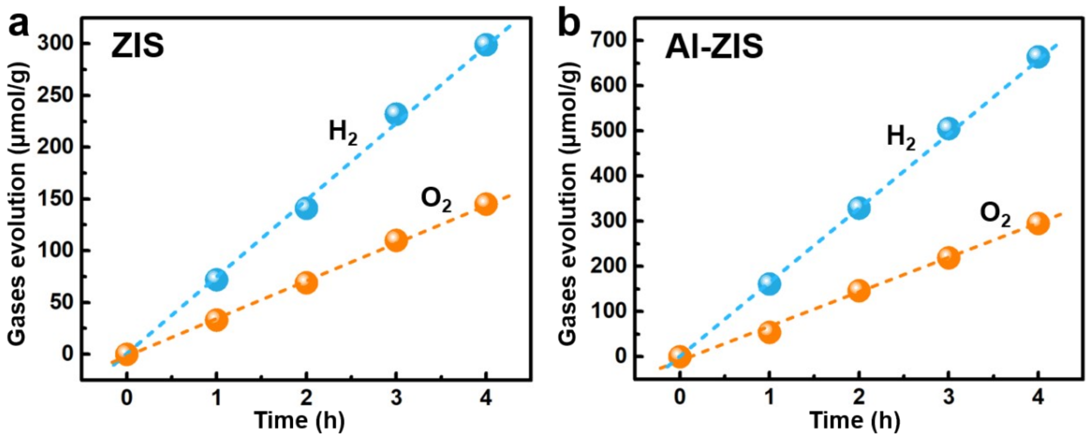

Fig. S9. Photocatalytic H_2 and O_2 evolution of ZIS and Al-ZIS nanosheets under AM1.5G.

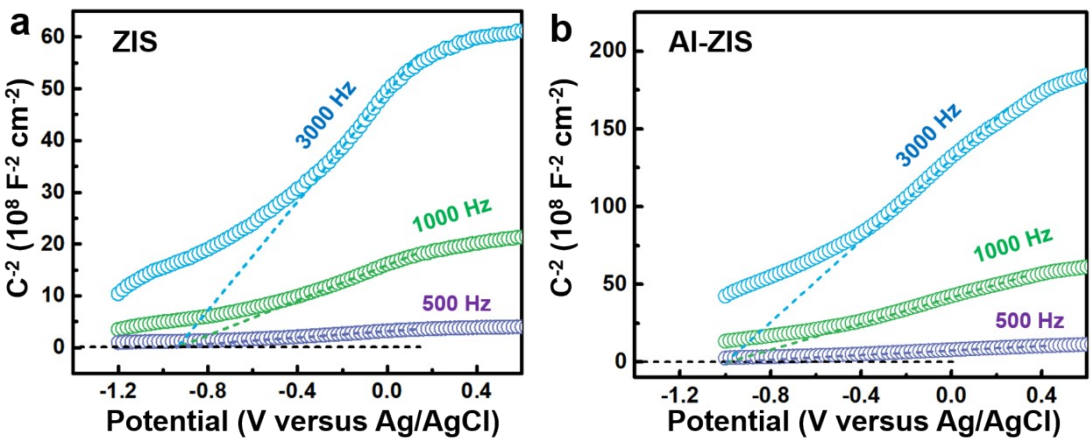

Fig. S10. Mott-Schottky plots of ZIS and Al-ZIS with different frequencies.

Table S1. The lattice constants of ZIS and Al-ZIS nanosheets.

Samples	Cell parameters (Å)			V (Å^3)	Rp (%)
	a	b	c		
ZIS	3.7245533	3.7245533	26.2388867	315.22773	7.06
Al-ZIS	3.7816752	3.7816752	30.6091280	379.09674	7.51

Table S2. Solar-driven overall water splitting performance of various photocatalysts in reported references.

Photocatalysts	Activity measurement			Ref.
	H_2 (μmol/g/h)	O_2 (μmol/g/h)	Illumination	
L-NiCo double hydroxide	34.0	16.8	300 W Xe lamp (AM1.5)	1
Ag- $ZnIn_2S_4$	56.6	29.1	300 W Xe lamp (>420 nm)	2
TiO_2-$ZnIn_2S_4$	214.9	81.7	300 W Xe lamp (full spectrum)	3
Pt-$ZnIn_2S_4$/rGO/Co_3O_4-$BiVO_4$	24.5	11.9	300 W Xe lamp (>420 nm)	4
ZIS-WO/C-wood	169.2	82.5	300 W Xe lamp (AM 1.5G)	5
MoS_2-CdS/WO_3-MnO_2	0.5	0.26	300 W Xe lamp (>420 nm)	6
PtS-$ZnIn_2S_4$/WO_3-MnO_2	38.8	15.7	300 W Xe lamp (>420 nm)	7
Single atom Ni/ Polymeric carbon nitride	26.7	24.0 (H_2O_2)	300 W Xe lamp (>420 nm)	8
CoO atomic layers	4.4	2.6	300 W Xe lamp (>420 nm)	9
PtO_x/WN	0.9	0.48	300 W Xe lamp (>420 nm)	10
Cu_2O	4.0	2.0	300 W Xe lamp (>460 nm)	11
Al-ZIS	**77.2**	**35.3**	**300 W Xe lamp (>420 nm)**	**This work**

Table S3. ICP-OES data for Al-ZIS with different amount of Al doping.

Samples	Atomic concentration (ppm)		
	Zn	In	Al
ZIS	8.21	42.38	0
Al-ZIS-1	7.46	41.03	0.27
Al-ZIS-2	8.13	42.29	0.48
Al-ZIS-3	8.60	43.53	0.59
Al-ZIS-4	8.27	42.51	0.77
Al-ZIS-5	8.16	41.38	1.58

Table S4. Parameters obtained from time-resolved PL decay curves according to a double-exponential decay.

Samples	τ_1 (ns)	τ_2 (ns)	A_1 (ns)	A_2 (ns)	τ_{av} (ns)
ZIS	0.89	6.11	54.62	45.38	5.33
Al-ZIS	0.72	7.58	41.22	58.78	7.15

References:

1. Wang, M.; Wang, J. Q.; Xi, C. et al. A Hydrogen Deficient Nickel-Cobalt Double Hydroxide for Photocatalytic Overall Water Splitting. Angew. Chem. Int. Ed. 2020, 132 (28), 11607-11612.
2. Pan, R.; Hu, M.; Liu, J. et al. Two-Dimensional All-in-One Sulfide Monolayers Driving Photocatalytic Overall Water Splitting, Nano Lett. 2021, 21, 6228-6236.
3. Zuo, G.; Wang, Y.; Teo, W. L. et al. Direct Z-scheme TiO_2-$ZnIn_2S_4$ nanoflowers for cocatalyst-free photocatalytic water splitting, Appl. Catal. B-Environ. 2021, 291, 120126.
4. Ou, M.; Li, J.; Geng, M. et al. Construction of Z-scheme Photocatalyst Containing $ZnIn_2S_4$, Co_3O_4-Photodeposited $BiVO_4$ (110) Facets and rGO Electron Mediator for Overall Water Splitting into H_2 and O_2, Catal. Lett. 2021, 151, 2570-2582.
5. Wang, Y.; Huang, W.; Guo, S. et al. Sulfur-Deficient $ZnIn_2S_4$/Oxygen-Deficient WO_3 Hybrids with Carbon Layer Bridges as a Novel Photothermal/ Photocatalytic Integrated System for Z-Scheme Overall Water Splitting, Adv. Energy Mater. 2021, 11, 2102452.
6. Wei, D.; Ding, Y.; Li, Z. Noble-metal-free Z-Scheme MoS_2-CdS/WO_3-MnO_2 nanocomposites for photocatalytic overall water splitting under visible light, Int. J. Hydrog. Energy 2020, 45, 17320-17328.
7. Ding, Y.; Wei, D.; He, R. et al. Rational design of Z-scheme PtS-$ZnIn_2S_4$/WO_3-MnO_2 for overall photocatalytic water splitting under visible light, Appl. Catal. B-Environ. 2019, 258, 117948.
8. Li, Y.; Wang, Y.; Dong, C. et al. Single-atom nickel terminating sp^2 and sp^3 nitride in polymeric carbon nitride for visible-light photocatalytic overall water splitting, Chem. Sci. 2021, 12, 3633-3643.
9. Xu, J.; Li, X.; Ju, Z. et al. Visible-Light-Driven Overall Water Splitting Boosted by Tetrahedrally Coordinated Blende Cobalt (II) Oxide Atomic Layers. Angew. Chem. Int. Ed. 2019, 131, 3064-3068.
10. Wang, Y.; Nie, T.; Li, Y. et al. Black Tungsten Nitride as a Metallic Photocatalyst for Overall Water Splitting Operable at up to 765 nm, Angew. Chem. Int. Ed. 2017, 56, 7430-7434.
11. Hara, M.; Kondo, T.; Komoda, M. et al. Cu_2O as A Photocatalyst for Overall Water Splitting under Visible Light Irradiation. Chem. Commun. 1998, 357-358.